THE ASTROPHYSICAL JOURNAL, 535:L13–L16, 2000 May 20

A COMPARISON OF ESTIMATORS FOR THE TWO-POINT CORRELATION FUNCTION

MARTIN KERSCHER,[1,2] ISTVÁN SZAPUDI,[3] AND ALEXANDER S. SZALAY[1]
Received 1999 December 2; accepted 2000 April 5; published 2000 May 23

ABSTRACT

Nine of the most important estimators known for the two-point correlation function are compared using a predetermined, rigorous criterion. The indicators were extracted from over 500 subsamples of the Virgo Hubble volume simulation cluster catalog. The "real" correlation function was determined from the full survey in a 3000 h^{-1} Mpc periodic cube. The estimators were ranked by the cumulative probability of returning a value within a certain tolerance of the real correlation function. This criterion takes into account bias and variance, and it is independent of the possibly non-Gaussian nature of the error statistics. As a result, for astrophysical applications, a clear recommendation has emerged: the Landy & Szalay estimator, in its original or grid version (Szapudi & Szalay), is preferred in comparison with the other indicators examined, with a performance almost indistinguishable from the Hamilton estimator.

Subject headings: galaxies: clusters: general — methods: statistical

1. INTRODUCTION

The two-point correlation function of galaxies became one of the most popular statistical tools in astronomy and cosmology. If the current paradigm, in which the initial Gaussian fluctuations grew by gravitational instability, is correct, the two-point correlation function of galaxies is directly related to the initial mass power spectrum. While the role of the two-point correlation function is central, estimators for extracting it from a set of spatial points are confusingly abundant in the literature. We have collected the nine most important forms used in the area of mathematics and astronomy. The difference between them lies mainly in their respective method of edge correction.

The multitude of choices might appear confusing to the practicing observational astronomer. The reason is partly due to the lack of a clear criterion to distinguish between the estimators. For instance, one estimator could have smaller variance under certain circumstances, but it could have a bias. Therefore, *before* doing any numerical experiments, we agreed on the method of ranking the different estimators. The cumulative probability distribution of the measured value lying within a certain tolerance of the "true" value is going beyond the concepts of bias or variance, and it even takes into account any non-Gaussian behavior of the statistics. This is the mathematical formulation of the simple idea that an estimator that is more likely to give values closer to the truth is better. After the above criterion was agreed on, the plan to elucidate the confusion was clear. We collect the different forms of estimators (§ 2) and perform a numerical experiment in several subsamples of a large simulation (§ 3), determining the cumulative probability of measuring values close to the true one and thereby ranking the different estimators (§ 4).

2. THE ESTIMATORS

Astrophysical studies favor estimators based on counting pairs, while most of the mathematical research is focused on geometric edge correction (§ 2.2). In the following subsections, we collect nine of the most successful and widespread recipes from both genres.

2.1. *Pairwise Estimators*

Following Szapudi & Szalay (1998), let us define the pair counts with a function Φ that is symmetric in its arguments:

$$P_{DR}(r) = \sum_{\boldsymbol{x}\in D}\sum_{\boldsymbol{y}\in R} \Phi_r(\boldsymbol{x},\boldsymbol{y}). \tag{1}$$

The summation runs over coordinates of points in the data set D and points in the set R of randomly distributed points, respectively. This Letter considers the two-point correlation function, for which the appropriate definition is $\Phi_r(\boldsymbol{x},\boldsymbol{y}) = [r \le d(\boldsymbol{x},\boldsymbol{y}) \le r + \Delta]$, where $d(\boldsymbol{x},\boldsymbol{y})$ is the separation of the two points and the condition in brackets equals 1 when the condition holds and 0 otherwise. P_{DD} and P_{RR} are defined analogously, with $\boldsymbol{x}$ and $\boldsymbol{y}$ taken entirely from the data and random samples, under the restriction that $\boldsymbol{x} \neq \boldsymbol{y}$. Let us introduce the normalized counts $DD(r) = P_{DD}(r)/[N(N-1)]$, $DR(r) = P_{DR}(r)/(NN_R)$, $RR(r) = P_{RR}(r)/[N_R(N_R-1)]$, with N and N_R being the total number of data and random points in the survey volume, respectively. With the above preparation, the pairwise estimators used in what follows are the natural estimator $\hat{\xi}_n$ and the estimators that are due to Davis & Peebles (1983; $\hat{\xi}_{\rm DP}$), Hewett (1982; $\hat{\xi}_{\rm Hew}$), Hamilton (1993; $\hat{\xi}_{\rm Ham}$), and Landy & Szalay (1993, hereafter LS; $\hat{\xi}_{\rm LS}$):

$$\hat{\xi}_n = \frac{DD}{RR} - 1,\ \hat{\xi}_{\rm DP} = \frac{DD}{DR} - 1,\ \hat{\xi}_{\rm Hew} = \frac{DD-DR}{RR},$$
$$\hat{\xi}_{\rm Ham} = \frac{DD\,RR}{DR^2} - 1,\ \hat{\xi}_{\rm LS} = \frac{DD-2DR+RR}{RR}. \tag{2}$$

Note that Hewett's estimator could be rendered equivalent to the LS estimator if the original asymmetric definition of DR is symmetrized; the version we use is the one that is consistent with the notation laid out above. In the case of an angular survey, an optimal weighting scheme can be adapted to any of the above estimators (e.g., Colombi, Szapudi, & Szalay 1998). This is inversely proportional to the errors expected at a particular pair separation, essentially equivalent to the Feldman, Kaiser, & Peacock (1994) weight.

[1] Department of Physics and Astronomy, Johns Hopkins University, Baltimore, MD 21218.
[2] Ludwig-Maximillians-Universität, Theresienstrasse 37, München, D-80333, Germany; kerscher@theorie.physik.uni-muenchen.de.
[3] Canadian Institute for Theoretical Astrophysics, University of Toronto, 60 St. George Street Toronto, Ontario, M5S 3H8, Canada.

TABLE 1
PARAMETERS FOR THE SAMPLES

PARAMETER	SAMPLES					
	C	**S**	**P**	**H**	**N**	**R1/R10**
L_{xy} (Mpc h^{-1})	375	1000	130	375	375	375
L_z (Mpc h^{-1})	375	52.6	3000	375	375	375
n_S	512	513	529	512	512	512
N	434	433	420	434	434	434
N_R	10^5	10^5	10^5	10^5	10^5	1000/10,000

NOTE.—L_{xy} and L_z are the side lengths of the rectangular samples, n_S is the number of samples exhausting the periodic cube with 222,052 clusters in total, N is the mean number of clusters inside the samples, and N_R is the number of random points used.

2.2. *Geometric Estimators*

Alternative estimates of the two-point correlation function from N data points $\boldsymbol{x} \in D$ inside a sample window $\mathcal{W}$ may be written in the form

$$\hat{\xi}(r) + 1 = \frac{|\mathcal{W}|}{N(N-1)} \sum_{\boldsymbol{x}\in D} \sum_{\boldsymbol{y}\in D} \frac{\Phi_r(\boldsymbol{x},\boldsymbol{y})}{4\pi r^2 \Delta}\, \omega(\boldsymbol{x},\boldsymbol{y}). \tag{3}$$

Here $|\mathcal{W}|$ is the volume of the sample window, and the sum is restricted to pairs of different points $\boldsymbol{x} \neq \boldsymbol{y}$. For a suitably chosen weight function $\omega(\boldsymbol{x},\boldsymbol{y})$, these edge-corrected estimators are approximately unbiased. Such weights are the Ripley (1976)/Rivolo (1986) weight $\omega_{\rm R}$, the Ohser & Stoyan (1981)/Fiksel (1988) weight $\omega_{\rm F}$, and the Ohser (1983) weight $\omega_{\rm O}$:

$$\omega_{\rm R}(\boldsymbol{x},\boldsymbol{y}) = \frac{4\pi r^2}{\text{area}\ [\partial\mathcal{B}_r(\boldsymbol{x}) \cap \mathcal{W}]}, \quad \omega_{\rm F}(\boldsymbol{x},\boldsymbol{y}) = \frac{|\mathcal{W}|}{\gamma_{\mathcal{W}}(\boldsymbol{x}-\boldsymbol{y})},$$
$$\omega_{\rm O}(\boldsymbol{x},\boldsymbol{y}) = \frac{|\mathcal{W}|}{\overline{\gamma_{\mathcal{W}}}(|\boldsymbol{x}-\boldsymbol{y}|)}, \tag{4}$$

where area $[\partial\mathcal{B}_r(\boldsymbol{x}) \cap \mathcal{W}]$ is the fraction of the surface area of the sphere $\mathcal{B}_r(\boldsymbol{x})$ with radius $r = |\boldsymbol{x}-\boldsymbol{y}|$ around $\boldsymbol{x}$ inside $\mathcal{W}$, the set covariance $\gamma_{\mathcal{W}}(\boldsymbol{z}) = |\mathcal{W} \cap \mathcal{W}_{\boldsymbol{z}}|$ is the volume of the intersection of the original sample $\mathcal{W}$ with the set $\mathcal{W}_{\boldsymbol{z}}$ shifted by $\boldsymbol{z}$, and $\overline{\gamma_{\mathcal{W}}}(r)$ is the isotropized set covariance. We will consider the estimators $\hat{\xi}_{\rm R}$, $\hat{\xi}_{\rm F}$, and $\hat{\xi}_{\rm O}$ based on these weights. A detailed description of these estimators may be found in Stoyan, Kendall, & Mecke (1995) and Kerscher (1999). The minus or reduced sample estimator, employing no weighting scheme at all, may be obtained by looking only at the $N^{(r)}$ points $D^{(r)}$, which are farther than r from the boundaries of $\mathcal{W}$:

$$\hat{\xi}_m(r) + 1 = \frac{|\mathcal{W}|}{N} \frac{1}{N^{(r)}} \sum_{\boldsymbol{x}\in D^{(r)}} \sum_{\boldsymbol{y}\in D} \frac{\Phi_r(\boldsymbol{x},\boldsymbol{y})}{4\pi r^2 \Delta}. \tag{5}$$

Estimators of this type are used by Sylos Labini, Montuori, & Pietronero (1998).

It can be shown that the natural estimator $\hat{\xi}_n$ is the Monte Carlo version of the Ohser estimator $\hat{\xi}_{\rm O}$. Similarly, the geometric counterparts of the LS and Hamilton estimators may be constructed (Kerscher 1999). This allowed us to cross-check our programs. Focusing on improved number density estimation, Stoyan & Stoyan (2000) also arrived at the geometrical version of the Hamilton estimator.

3. THE COMPARISON

To compare these estimators for typical cosmological situations, we use the cluster catalog generated from the ΛCDM Hubble volume simulation (Colberg et al. 1998). In order to investigate the effects of shape, clustering, and the amount of random data used, we have always varied one parameter at a time, starting from a fiducial sample. Rectangular subsamples were extracted by exhausting the full simulation cube: the fiducial cubic subsamples **C**, slices **S**, pencil beams **P**, and cubic samples with cut-out holes **H**, all with approximately the same volume and with approximately 430 clusters each. Cut-out holes around bright stars, etc., arise naturally in all realistic surveys. The pattern of holes used for this study was directly mapped from a 19° × 19° patch of the Edinburgh/Durham Southern Galaxy Catalogue survey to one of the faces of the simulation subcube. Then the holes were continued across the subsample, parallel with the sides corresponding to a distant observer approximation. The physical size of the holes roughly corresponded to a redshift survey at a depth of about 300 h^{-1} Mpc. All these point sets are "fully sampled" and may be considered as volume-limited samples.

In addition, Poisson samples **N**, i.e., those without clustering, were generated. All calculations employed N_R = 100,000 random points for the pairwise estimators, unless otherwise noted. This was sufficient for all indicators to converge. The calculations were repeated for sample **C** with N_R = 1000 and N_R = 10,000 random points, denoted with **R1** and **R10**, respectively, to investigate the speed of convergence of the different estimators with respect to the random point density. The parameters for the samples are summarized in Table 1.

The two-point correlation function $\xi_{\rm per}$ extracted from all clusters inside the 3 h^{-1} Gpc cube provided our reference or "true value." Since the simulation was carried out with periodic boundary conditions, the cluster distribution is also periodic; therefore, the torus boundary correction is exact (Ripley 1988).

The nine estimators defined above for the two-point correlation function were determined from each of the n_S subsamples. For a given radial bin r, we computed the deviation $|\hat{\xi}_\star(r) - \xi_{\rm per}(r)|$ of the estimated two-point correlation function $\hat{\xi}_\star(r)$ from the reference $\xi_{\rm per}(r)$. The empirical distribution of these deviations provides an objective basis for the comparison of the utility of the estimators. The large number of samples enabled the numerical estimation of the probability $P(|\hat{\xi}_\star - \xi_{\rm per}| < d)$ that the deviation $|\hat{\xi}_\star - \xi_{\rm per}|$ is smaller than a tolerance d. The larger this probability, the more likely that the estimator will be within the predetermined range from one sample. In general, it could happen that the rank of two estimators reverses as the tolerance varies, but as will be shown in the next section, this is quite atypical. This procedure is more general than considering only bias and variance, which yields only a full description if the above distribution is the integral of a Gaussian. Note that a small bias is negligible for practical purposes if the variance dominates the distribution of the deviations. It is worthwhile to note that the Gaussian assumption yields a surprisingly good description of the deviations $|\hat{\xi}_\star(r) - \xi_{\rm per}(r)|$. For estimators of the closely related product density, asymptotic Gaussianity of the deviations was proved by Heinrich (1988).

Figure 1 shows the distribution $P\,[|\hat{\xi}_\star(r) - \xi_{\rm per}(r)| < d]$ for the samples described in Table 1. Three typical scales are displayed to illustrate the general behavior. The principal conclusions to be drawn are the following:

Small scales (r = 4.4 h^{-1} Mpc).—The effect of any bound-

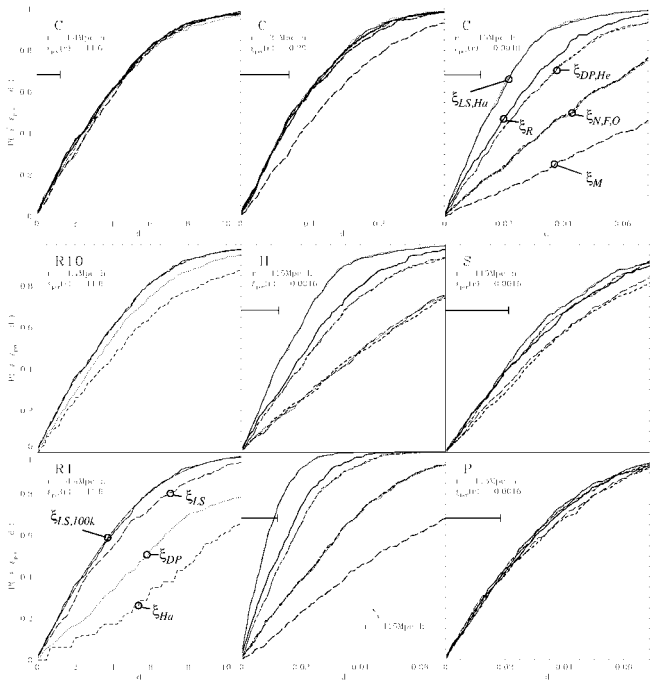

FIG. 1.—Cumulative probability distribution $P\,[\,|\hat{\xi}_{\star}(r) - \xi_{\rm per}(r)| < d]$ of the deviations d shown for several samples and radii r. In the plots for the samples **C**, **S**, **P**, **H**, and **N**, we use the following symbols for the deviations of the estimators: natural (*long-dashed line*), Davie-Peebles (*dot-dashed line*), Hewett (*short-dashed line*), Hamilton (*dotted line*), LS (*solid line*), Rivolo (*thick solid line*), Fiksel (*thick dotted line*), Ohser (*thick short-dashed line*), and minus (*thick long-dashed line*). (On large scales, neither the minus estimator nor the Fiksel estimater are applicable in the samples **S** and **P**, and consequently no results for them are shown.) The horizontal lines starting at 0.683 mark the value of $\sigma_{\rm LS}$ for a Poisson process, according to eq. (6) in the geometry considered. In the plots for **R1** and **R10**, the solid line marks the result for the LS estimator using 100,000 points. The estimators using 1000 and 10,000 random points, respectively, are marked in the following way: Davis-Peebles (*dotted line*), Hamilton (*short-dashed line*), and LS (*long-dashed line*). For better visibility, we laid a Gaussian distance distribution (*dot-dashed line*) over the result for the LS estimator only in the plot for R1. A similar perfect agreement would be obtained in the other cases.

ary correction scheme becomes negligible, and as expected, all the estimators exhibit nearly identical behavior. The same is true for the samples **S**, **P**, **N**, and **H** not shown. However, some of the estimators are more sensitive to the density of random points, especially the Hamilton estimator, followed by the Davis-Peebles estimator. They show stronger deviations for the **R1** and **R10** samples because of the poor sampling of the *DR* term (see also Pons-Bordería et al. 1999). This effect persists on large scales as well.

Intermediate scales ($r = 31\ h^{-1}$ Mpc).—These scales are similar to the small scales, but the minus estimator shows stronger deviation, becoming even more pronounced for the **S**, **P**, and **H** samples since the effective remaining volume decreases.

Large scales ($r = 115\ h^{-1}$ Mpc).—Edge corrections are becoming important, and the estimators exhibit clear differences in their distributions of the deviations for the samples **C** and **N**. For a given probability, the minus estimator shows the largest deviations, followed by the natural, Fiksel, and Ohser estimators. Significantly smaller deviations are obtained for the Davis-Peebles and Hewett estimators, and yet they are smaller for the Rivolo estimator. Finally, the Hamilton and LS estimator display the smallest deviations and thus the best edge correction. The two latter distributions nearly overlap. The above conclusions are robust and only weakly influenced by the presence of cut-out holes, as seen from the **H** sample. The geometry of the subsamples has a nontrivial effect on the distributions. While the deviations are increased in the **S** and **P** samples, the differences between the estimators are reduced in the **S** samples, becoming negligible in the **P** samples. In both cases, the minus estimator is not usable any more since the $N^{(r)}$ equal zero, whereas the Fiksel estimator is biased for such geometries on large scales (this is implicitly shown in the work of Ohser 1983).

Following Szapudi & Szalay (2000), the variance of the LS estimator may be calculated for a Poisson process:

$$\sigma^2_{\rm LS}(r) = \frac{2}{V_{\Delta}(r)\overline{\rho}^2}\,, \tag{6}$$

with $V_{\Delta}(r) = \int_{\mathcal{W}} d^3x \int_{\mathcal{W}} d^3y\ \Phi_r(\boldsymbol{x}, \boldsymbol{y})$. The $\sigma_{\rm LS}$ calculated for the considered samples is also shown in Figure 1 to illustrate how much discreteness effects contribute to the distribution of the deviations. For our choice of sample parameters, the discreteness contribution, i.e., the deviation of a corresponding Poisson sample, is always within a factor of a few other important contributions to the variance, such as the finite volume and edge effects. In general, the ratio of discreteness effects to the full variance depends, in a complicated nonlinear fashion, on the number of clusters in the sample, the shape of the survey, the integrals over the two-point correlation function and its square, and the three- and four-point correlation functions (I. Szapudi, S. Colombi, & A. S. Szalay 2000, in preparation). Varying the side length of the cubic samples from 300, 375, and 600 h^{-1} Mpc to 1 h^{-1} Gpc, we explored the influence of the size of the sample on the discreteness effects. Still, the rank order of the estimators stayed invariant.

4. SUMMARY AND CONCLUSION

For a sample with 222,052 clusters extracted from the Virgo Hubble volume simulation, a reference two-point correlation function was determined. Within over 500 subsamples, several estimators for the two-point correlation function were employed, and the results were compared with the reference value. On small scales, all the estimators are comparable. On large scales, the LS estimator and the Hamilton estimator significantly outperform the rest, showing the smallest deviations for a given cumulative probability. While the two estimators yield almost identical results for an infinite number of random points, the Hamilton estimator is considerably more sensitive to the number of random points employed than the LS version is. From a practical point of view, the LS estimator is thus preferable. The rest of the estimators can be divided into three categories. The first runner-ups are the estimators from Rivolo, Davis-Peebles, and Hewett, but already with a significantly increased variance. Even larger deviations are present for the natural, Fiksel, and Ohser recipes. The minus estimator has the largest deviation. Although it was shown that for special point processes, both the LS and Hamilton estimator are biased (Kerscher 1999), the present numerical experiment demonstrates that this is irrelevant for the realistic galaxy and cluster point processes since the bias has an insignificant effect on the distribution of deviations. Pons-Bordería et al. (1999) did not recommend one estimator for all cases. In contrast, through

our extensive numerical treatment, the LS estimator emerges as the one we clearly recommend.

The above considerations apply to volume-limited samples. When the correlation function is estimated directly from a flux-limited sample with an appropriate minimum variance pair weighting (Feldman et al. 1994), the Hamilton estimator has the advantage of being independent of the normalization of the selection function.

The differences between the estimators become smaller for the slice samples and insignificant for the pencil-beam samples. At first sight, this is counterintuitive: the difference between the estimators is largely due to edge corrections, and less compact surveys obviously have more edges. For the large scale considered, **S** and **P** become essentially two- and one-dimensional, respectively, and the weight $\omega(\boldsymbol{x}, \boldsymbol{y}) \approx \bar{\omega}(r)$ is equal for most of the pairs separated by r. Since the geometric estimators are approximately unbiased, they employ mainly the same weight $\bar{\omega}(r)$ on large scales and consequently show the same distribution of deviations. This argument also applies to the pair estimators since they may be written in terms of these weights (Kerscher 1999).

All the above numerical investigations are intimately related to the problem of calculating the expected errors on estimators for correlation functions. To include all contributions, such as edge, discreteness, and finite-volume effects, the method by Colombi, Bouchet, & Schaeffer (1994), Szapudi & Colombi (1996), Colombi et al. (1998), and Szapudi, Colombi, & Bernardeau (1999) has to be extended for the two-point correlation function. Such a calculation was performed by I. Szapudi, S. Colombi, & A. S. Szalay (2000, in preparation; see Stoyan, Bertram, & Wendrock 1993, Bernstein 1994, and Hamilton 1993 for approximations) and should be used for ab initio error calculations.

It is worth mentioning that one of the most widely used methods in the literature, i.e., "bootstrap," is based on a misunderstanding of the concept. For bootstrap in spatial statistics, a *whole* sample takes the role of one point in the original bootstrap procedure. This means that replicas of the original surveys would be needed to fulfill the promise of the bootstrap method. Choosing *points* (i.e., individual galaxies, clusters, etc.) randomly from one sample, as is usually done, yields a variance with no obvious relation to the variance sought (see also Snethlage 1999).

The role of the random samples is to represent the shape of the survey in a Monte Carlo fashion. A practical alternative is to put a fine grid on the survey and calculate the quantities *DD*, *DW*, and *WW*, where *D* now represents bin counts and *W* represents the indicator function, taking the value of 1 for pixels inside the survey and 0 otherwise. According to Szapudi & Szalay (1998), all the above estimators have an analogous "grid" version (see also Hamilton 1993) that can be obtained formally by the substitution $R \rightarrow W$. In practice, grid estimators can be more efficient than pair counts, and except for a slight perturbation of the pair-separation bins, they both yield almost identical results for scales larger than a few pixel size.

The usual way of estimating the power spectrum, using a folding with the Fourier transform of the sample geometry, is equivalent to the grid version of the LS estimator. Hence, such a power spectrum analysis extracts the same amount of information from the data as the analysis with the two-point correlation function that uses the grid version of the LS estimator. The results are only displayed with respect to a different basis. Similarly, Karhunen-Loève (KL) modes form another set of basis functions (Vogeley & Szalay 1996). The uncorrelated power spectrum (Hamilton 2000) and the KL modes are the methods of choice for the cosmological parameter estimation. The KL modes allow for a well-defined cutoff and therefore reduce the computational needs in a maximum likelihood analysis. However, geometrical features of the galaxy and cluster distribution show up directly in the two-point correlation function and may be interpreted easily. Each bin of the two-point correlation function contains direct information on pairs separated by a certain distance; this is an intuitively simple concept that is more suitable to the study and control (expected or unexpected) of systematics (geometry, luminosity, galaxy properties, biases) than any other representation. In this sense, the correlation function is a tool that is complementary to the power spectrum.

We are grateful to the Virgo Supercomputing Consortium,[4] who made the Hubble volume simulation data available for our project. The simulation was performed on the T3E at the Computing Centre of the Max-Planck Society in Garching. We would like to thank Simon White and the referee Andrew Hamilton for useful suggestions and discussions. M. K. would like to thank Claus Beisbart and Dietrich Stoyan for interesting and helpful discussions. I. S. was supported by the PPARC rolling grant for Extragalactic Astronomy and Cosmology at Durham while there. M. K. acknowledges support from the Sonderforschungsbereich für Astroteilchenphysik SFB 375 der DFG. A. S. Szalay has been supported by the NSF (AST 98-02980) and NASA LTSA (NAG6-53503).

[4] See http://star-www.dur.ac.uk/~frazerp/virgo/virgo.html.

REFERENCES

Bernstein, G. M. 1994, ApJ, 424, 569
Colberg, J. M., et al. 1998, in Wide Field Surveys in Cosmology, ed. S. Colombi & Y. Mellier (Château de Blois: Editions Frontières), 247
Colombi, S., Bouchet, F., & Schaeffer, R. 1994, A&A, 281, 301
Colombi, S., Szapudi, I., & Szalay, A. S. 1998, MNRAS, 296, 253
Davis, M., & Peebles, P. J. E. 1983, ApJ, 267, 465
Feldman, H. A., Kaiser, N., & Peacock, J. A. 1994, ApJ, 426, 23
Fiksel, T. 1988, Statistics, 19, 67
Hamilton, A. J. S. 1993, ApJ, 417, 19
———. 2000, MNRAS, 312, 257
Heinrich, L. 1988, Statistics, 19, 87
Hewett, P. C. 1982, MNRAS, 201, 867
Kerscher, M. 1999, A&A, 343, 333
Landy, S. D., & Szalay, A. S. 1993, ApJ, 412, 64 (LS)
Ohser, J. 1983, Math. Operationsforsch. u. Statist., Ser. Statist., 14, 63
Ohser, J., & Stoyan, D. 1981, Biometrical J., 23, 523
Pons-Bordería, M.-J., Martínez, V. J., Stoyan, D., Stoyan, H., & Saar, E. 1999, ApJ, 523, 480
Ripley, B. D. 1976, J. Appl. Prob., 13, 255
———. 1988, Statistical Inference for Spatial Processes (Cambridge: Cambridge Univ. Press)
Rivolo, A. R. 1986, ApJ, 301, 70
Snethlage, M. 1999, Metrika, 49, 245
Stoyan, D., Bertram, U., & Wendrock, H. 1993, Ann. Inst. Satist. Math., 45, 211
Stoyan, D., Kendall, W. S., & Mecke, J. 1995, Stochastic Geometry and Its Applications (Chichester: Wiley)
Stoyan, D., & Stoyan, H. 2000, Scand. J. Satist., in press
Sylos Labini, F., Montuori, M., & Pietronero, L. 1998, Phys. Rep., 293, 61
Szapudi, I., & Colombi, S. 1996, ApJ, 470, 131
Szapudi, I., Colombi, S., & Bernardeau, F. 1999, MNRAS, 310, 428
Szapudi, I., & Szalay, A. S. 1998, ApJ, 494, L41
———. 2000, Annales de l'ISUP, in press
Vogeley, M. S., & Szalay, A. S. 1996, ApJ, 465, 34